JACS JOURNAL OF THE AMERICAN CHEMICAL SOCIETY

Communication

Cite This: J. Am. Chem. Soc. 2018, 140, 16418−16422

pubs.acs.org/JACS

Photoreduction of CO_2 with a Formate Dehydrogenase Driven by Photosystem II Using a Semi-artificial Z-Scheme Architecture

Katarzyna P. Sokol,[†,⊥] William E. Robinson,[†,⊥] Ana R. Oliveira,[‡] Julien Warnan,[†] Marc M. Nowaczyk,[§] Adrian Ruff,[∥] Inês A. C. Pereira,[‡] and Erwin Reisner*[,†]

[†]Department of Chemistry, University of Cambridge, Lensfield Road, Cambridge CB2 1EW, U.K.

[‡]Instituto de Tecnologia Química e Biológica António Xavier (ITQB NOVA), Universidade NOVA de Lisboa, Av. da República, 2780-157 Oeiras, Portugal

[§]Plant Biochemistry, Faculty of Biology & Biotechnology, Ruhr-Universität Bochum, Universitätsstraße 150, 44780 Bochum, Germany

[∥]Analytical Chemistry - Center for Electrochemical Sciences, Faculty of Chemistry and Biochemistry, Ruhr-Universität Bochum, Universitätsstraße 150, 44780 Bochum, Germany

Supporting Information

ABSTRACT: Solar-driven coupling of water oxidation with CO_2 reduction sustains life on our planet and is of high priority in contemporary energy research. Here, we report a photoelectrochemical tandem device that performs photocatalytic reduction of CO_2 to formate. We employ a semi-artificial design, which wires a W-dependent formate dehydrogenase (FDH) cathode to a photoanode containing the photosynthetic water oxidation enzyme, Photosystem II, via a synthetic dye with complementary light absorption. From a biological perspective, the system achieves a metabolically inaccessible pathway of light-driven CO_2 fixation to formate. From a synthetic point of view, it represents a proof-of-principle system utilizing precious-metal-free catalysts for selective CO_2-to-formate conversion using water as an electron donor. This hybrid platform demonstrates the translatability and versatility of coupling abiotic and biotic components to create challenging models for solar fuel and chemical synthesis.

In the thylakoid membrane of plants, light-driven water oxidation in the photosynthetic Z-scheme is coupled to CO_2 fixation for sugar synthesis via the dark Calvin−Benson−Bassham (CBB) cycle (eq 1).[1,2] Although this solar-energy-storing reaction is one of the most fundamental processes in biology and essential for life, it also exemplifies the inefficiencies of solar-to-fuel conversion.[3] For example, Photosystem II (PSII) and Photosystem I (PSI) are non-complementary light absorbers, which limits light harvesting efficiency. Ribulose-1,5-bisphosphate carboxylase/oxygenase (RuBisCO) is responsible for CO_2 fixation but has low turnover rates (1−10 s^{-1}), thereby creating a significant kinetic bottleneck. RuBisCO also reacts with O_2 to produce 2-phosphoglycolate, which must be recycled in energy-demanding, CO_2-evolving photorespiration.[4,5] The CBB cycle involves significant adenosine triphosphate (ATP) consumption, which leads to a lower biomass production efficiency compared to the prokaryotic reductive acetyl-coenzyme A (rAcCoA) pathway.[6] This alternative, light-independent route to CO_2 fixation uses the energy vector hydrogen as electron donor to reduce two CO_2 molecules to acetate in a linear sequence of reaction steps.[7]

$$6CO_2 + 6H_2O + 48h\nu \rightarrow C_6H_{12}O_6 + 6O_2 \quad (1)$$

Addressing the limitations of biological carbon fixation presents several challenges,[8−14] leading research toward *in vitro* (but light-independent) carbon fixation pathways.[15] As a bio-inspired alternative, artificial photosynthesis aspires to couple solar-light-driven water oxidation with CO_2 reduction to chemical fuels at higher efficiency than natural systems.[16] However, artificial photosynthetic carbon fixation is currently not economically feasible due to a lack of efficient, selective, or inexpensive catalysts and light absorbers.[17]

One of the entry points of CO_2 into the rAcCoA pathway is its conversion to formate before transfer to tetrahydrofolate (the second entry point involves its reduction to CO by carbon monoxide dehydrogenase/AcCoA synthase).[7] Coupling this process to light-driven water oxidation is a compelling step toward creating an efficient, artificial photosynthetic carbon fixation pathway. Formate is also a stable intermediate between CO_2 and methanol/methane, a hydrogen carrier, and a viable fuel itself.[18,19] Semi-artificial photosynthesis, in which catalytically efficient redox enzymes are interfaced with synthetic materials, offers a possibility to couple this key entry point of the rAcCoA pathway to light-driven CO_2 reduction and bypasses the energy-demanding and inefficient use of ATP.

Mo- and W-dependent formate dehydrogenases (FDHs) are enzymes capable of interconverting CO_2 and formate.[20−28] When adsorbed on an electrode, FDHs from *Syntrophobacter fumaroxidans*[21] and *Escherichia coli*[24,28] have been shown to perform reversible electrocatalysis with high efficiency through fast interfacial electron transfer. The activity of a Mo-FDH from *E. coli* has been harnessed in fuel cell devices, in which it was immobilized in cobaltocene- and viologen-functionalized

Received: September 21, 2018
Published: November 19, 2018

redox polymers.[29,30] Electrochemical CO_2 reduction using a W-FDH has been reported in mediated[31,32] and unmediated systems.[27] These FDHs contrast with metal-independent FDHs, which reduce CO_2 using nicotinamide adenine dinucleotide (NADH), an unstable, expensive, and diffusive cofactor with little driving force.[33−42] Metal-independent FDHs have been coupled to molecular,[43−46] biological,[47,48] and solid-state[38,41] visible-light-absorbers. In addition to the limitations of NADH utilization, these systems suffer from low selectivity and rely on sacrificial electron donors.

Here, we report a semi-artificial photoelectrochemical (PEC) tandem cell that wires the enzymes PSII and FDH to perform light-driven CO_2 conversion to formate using water as an electron donor (eq 2). First, we study the CO_2 reduction

$$2CO_2 + 2H_2O + 8h\nu \rightarrow 2HCO_2^- + O_2 + 2H^+ \qquad (2)$$

activity of W-FDH from *Desulfovibrio vulgaris*[49] adsorbed on a hierarchically structured inverse opal titanium dioxide (IO-TiO_2) scaffold (IO-TiO_2|FDH). This IO-TiO_2|FDH cathode is then wired to a recently reported PSII-based dye-sensitized photoanode, IO-TiO_2|dpp|P_{Os}-PSII,[50] which combines isolated PSII from *Thermosynechococcus elongatus*, dpp (a phosphonated diketopyrrolopyrrole dye), and P_{Os} [poly(1-vinylimidazole-*co*-allylamine)-[Os(bipy)$_2$Cl]Cl redox polymer] to realize a light-driven rAcCoA pathway by coupling selective CO_2 fixation to light-driven water oxidation (Figure 1).

In this enzyme-catalyzed PEC system, photogenerated electrons in PSII, which is embedded in the redox polymer P_{Os}, are transferred to the electron acceptor plastoquinone B

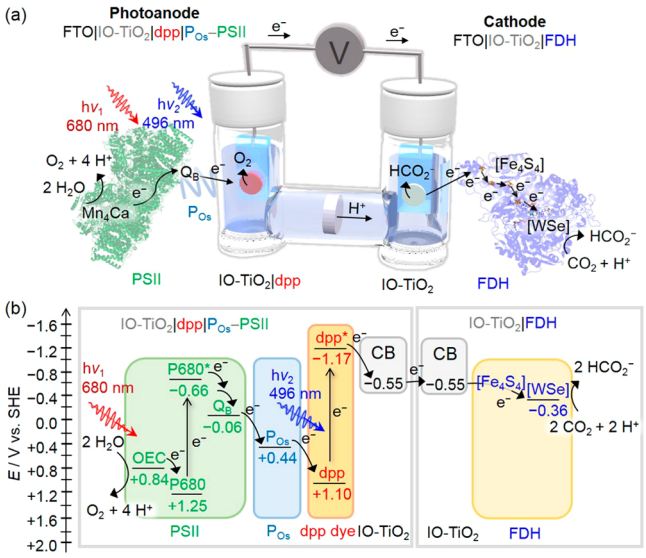

Figure 1. (a) Schematic representation of the semi-artificial photosynthetic tandem PEC cell coupling CO_2 reduction to water oxidation. A blend of P_{Os} and PSII adsorbed on a dpp-sensitized photoanode (IO-TiO_2|dpp|P_{Os}-PSII) is wired to an IO-TiO_2|FDH cathode (species size not drawn to scale). (b) Energy level diagram showing the electron-transfer pathway between PSII, the redox polymer (P_{Os}), the dye (dpp), the conduction band (CB) of IO-TiO_2 electrodes, four [Fe_4S_4] clusters, and the [WSe]-active site in FDH. All potentials are reported vs SHE at pH 6.5. Abbreviations: Mn_4Ca, oxygen-evolving complex (OEC); P680, pigment/primary electron donor; Q_B, plastoquinone B; [Fe_4S_4], iron−sulfur clusters; [WSe], FDH active site.

(Q_B, Figure S1). The holes are collected at the oxygen-evolving complex (OEC), where water is oxidized to liberate protons and gaseous O_2. The Os^{3+} complex in P_{Os} mediates electron transfer between reduced Q_B and oxidized dpp^+. The conduction band (CB) of IO-TiO_2 receives electrons from the photoexcited dpp*.[50] Electrons are transferred through the external electrical circuit to the IO-TiO_2|FDH cathode and arrive at the CO_2-reducing [WSe]-active site via interfacial electron transfer from the TiO_2 CB to iron−sulfur clusters (Fe_4S_4) which connect the FDH active site to its surface.

Hierarchical macro-mesoporous IO-TiO_2 electrodes (20 μm film thickness; geometrical surface area, A = 0.25 cm^2) were assembled on a fluorine tin oxide (FTO)-coated glass substrate (see Supporting Information).[50] An FDH solution (2 μL, 17 μM with 50 mM DL-dithiothreitol, incubated for 10 min) was drop-cast onto IO-TiO_2 to give the IO-TiO_2|FDH cathode. Anaerobic conditions were employed due to possible O_2 inhibition of FDH and side reactions of the electrode components with O_2. Protein film voltammetry (PFV) of IO-TiO_2|FDH in a solution of CO_2/$NaHCO_3$ (100 mM, pH 6.5, under 1 atm CO_2) and KCl (50 mM) demonstrated the high CO_2 reduction activity of the electrode (Figure 2). The current density (J) of IO-TiO_2|FDH was measured as a function of an applied potential (E_{app}) in a three-electrode configuration. The onset potential for CO_2 reduction to formate was observed close to the thermodynamic potential of the CO_2/HCO_2^- couple (−0.36 V vs standard hydrogen electrode, SHE) at approximately −0.4 V vs SHE, and a current density of −240 μA cm^{-2} was reached at −0.6 V vs SHE.

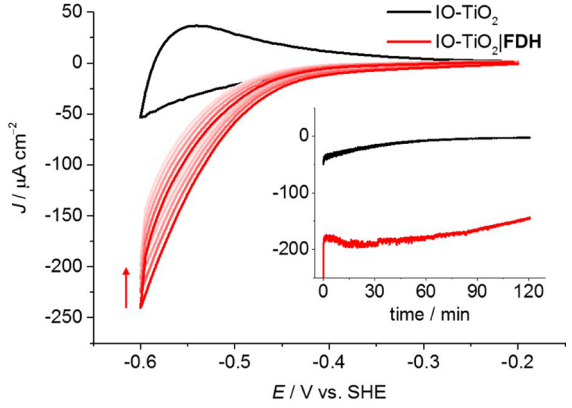

Figure 2. PFV scans (ν = 5 mV s^{-1}) of IO-TiO_2 (black trace) and IO-TiO_2|FDH (red traces, arrow indicates scan order). Inset: CPE at E_{app} = −0.6 V vs SHE. Conditions: CO_2/$NaHCO_3$ (100 mM), KCl (50 mM), 1 atm CO_2, pH = 6.5, T = 25 °C, continuous stirring. The three-electrode configuration employed a two-compartment cell with Ag/AgCl (saturated KCl) reference and Pt mesh counter electrodes.

The IO-TiO_2|FDH electrode exhibited good stability, retaining approximately 83% of its initial activity after controlled-potential electrolysis (CPE) for 2 h at E_{app} = −0.6 vs SHE (Figure 2, inset). The Faradaic efficiency (η_F) of formate production was determined as (78 ± 8)% (2.22 ± 0.23 μmol cm^{-2}). A voltammogram recorded immediately after the CPE experiment indicated electrode behavior similar to that measured before CPE (Figure S2), though with slightly lower, yet stable, activity. No H_2 production was detectable by gas chromatography (GC) analysis of the cell headspace, suggesting that the background current was due to charging

DOI: 10.1021/jacs.8b10247
J. Am. Chem. Soc. 2018, 140, 16418−16422

of the CB of TiO_2 (Figure 2).[51] The relatively high current densities of the IO-TiO_2|FDH electrode were likely due to high enzyme loading and effective wiring inside the porous, hierarchically structured IO-TiO_2 scaffold.[52,53] Thus, the cathode proved to be suitable for coupling to PSII-catalyzed water oxidation in a two-electrode PEC setup.

The activity of the IO-TiO_2|dpp|P_{Os}-PSII electrode in CO_2/$NaHCO_3$/KCl electrolyte solution was measured by stepped-potential chronoamperometry under periodic simulated solar illumination (Figure S3), showing behavior comparable to that of the recently reported PSII-modified dye-sensitized photoanode.[50] The photoanode was electrically wired to the IO-TiO_2|FDH cathode via a potentiostat, and the two electrodes were placed in compartments separated by a glass frit membrane in a PEC cell (Figure 1).

Stepped-voltage chronoamperometry under periodic illumination with UV-filtered simulated solar light (AM1.5G; irradiance E_e = 100 mW cm^{-2}; λ > 420 nm, Figure 3a) was used to study the system's performance. Upon irradiation, a current density of 5.5 ± 0.4 μA cm^{-2} was observed at zero applied voltage (U_{app}) (Figures S4 and S5). Voltage-independent steady-state photocurrents (99 ± 4 μA cm^{-2}) were reached at U_{app} > 0.4 V. Control experiments showed that small background responses were also observed using PSII-free IO-TiO_2|dpp photoanodes (Figure 3, green and black traces) due to electron transfer from photoexcited dpp to TiO_2 without dye regeneration, resulting in photobleaching.[50] When FDH was omitted from the system (Figure 3, blue trace), lower photoresponses were observed than in its presence, but the current response was higher than those responses observed in the absence of PSII. This background current is likely due to high capacitance of the high surface area IO-TiO_2 (charging of TiO_2 CB), supported by the cathodic discharging spikes observed upon switching off the light and persisting photocurrents in the chronoamperometry measurements with longer irradiation time (Figure S6). Substantial capacitance currents over a long time scale consistent with those observed in this study have been previously observed for porous TiO_2 electrodes.[51,54] At lower applied voltages (U_{app} < 0.4 V), Faradaic current from CO_2 reduction with FDH and some charging of TiO_2 should dominate, whereas at higher applied voltages (U_{app} > 0.5 V), substantial TiO_2 CB charging and possibly electrode degradation (e.g., FTO breakdown) could become significantly competing processes (Figure S7).

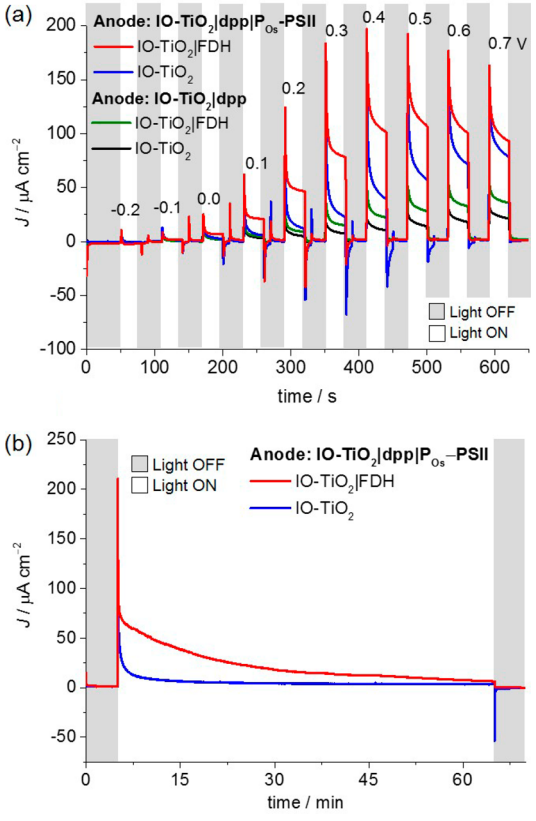

Figure 3. Characterization of two-electrode PEC cell consisting of IO-TiO_2|FDH cathode wired to IO-TiO_2|dpp|P_{Os}-PSII tandem photoanode. (a) Representative stepped-voltage chronoamperometry (0.1 V voltage steps with 30 s dark and 30 s light cycles) of the fully assembled PEC cell (red trace). Control experiments in the absence of PSII (green and black traces) and without FDH (blue and black traces) are also shown. Applied voltage (U_{app}) values are shown on top of the traces. (b) CPE (U_{app} = 0.3 V) of the two-electrode PSII-FDH system (red trace) and a similar system in the absence of FDH (blue trace). Conditions: CO_2/$NaHCO_3$ (100 mM), KCl (50 mM), 1 atm CO_2, pH = 6.5, T = 25 °C, continuous stirring. Simulated solar light source: AM 1.5G filter; E_e = 100 mW cm^{-2}; λ > 420 nm.

Only a small bias was required to drive the overall reaction (eq 2). CPE at U_{app} = 0.3 V with the IO-TiO_2|dpp|P_{Os}-PSII|| IO-TiO_2|FDH PEC cell under illumination was performed (Figure 3b). The photocurrent decayed from 92 to 7 μA cm^{-2} after 1 h irradiation with a half-life time ($\tau_{1/2}$) of ~8 min (Figure S8). Prolonged irradiation resulted in an irreversible drop in photocurrent, most likely due to PSII photodegradation.[3] Formate was detected (0.185 ± 0.017 μmol cm^{-2}) with η_F = (70 ± 6)%, but reliable O_2 analysis (estimated 0.132 μmol cm^{-2}, 0.01% O_2, assuming quantitative η_F) was prevented by the detection limit of the apparatus. Other products such as H_2 and CO could not be detected in the cathodic chamber. No products (H_2, CO, and formate) were observed in control experiments omitting FDH at U_{app} = 0.3 and 0.6 V (Figures 3b and S7).

In summary, we have demonstrated that the IO-TiO_2|dpp|P_{Os}-PSII||IO-TiO_2|FDH PEC cell achieves the biologically and synthetically challenging coupling of solar-driven water oxidation to selective CO_2 reduction with a small additional supply of energy (applied voltage) under mild conditions. The semi-artificial architecture employs efficient enzymes and synthetic components that enable not only complementary light absorption but also the coupling of unnatural redox partners, which is challenging *in vivo*. The PSII-FDH tandem PEC system reported here demonstrates how semi-artificial photosynthesis is a translatable and versatile platform, allowing a variety of electroactive enzymes to be studied electrochemically to gain a better understanding of their activity *in vitro*. From a biological perspective, this system can be viewed as an effective model for an engineered light-driven rAcCoA pathway that bypasses limitations of the natural Z-scheme and CBB cycle. Further biologically relevant electrochemical reactions and redox proteins may be coupled using this approach to introduce a plethora of model systems which extend solar-driven CO_2 reduction to production of value-added chemicals.

DOI: 10.1021/jacs.8b10247
J. Am. Chem. Soc. 2018, 140, 16418−16422

■ ASSOCIATED CONTENT

Supporting Information

The Supporting Information is available free of charge on the ACS Publications website at DOI: 10.1021/jacs.8b10247.

Materials and experimental methods for the electrode preparation, electrochemistry measurements (PFV, CPE, and PEC), and product analysis, including Figures S1–S8 (PDF)

■ AUTHOR INFORMATION

Corresponding Author

*reisner@ch.cam.ac.uk

ORCID

Erwin Reisner: 0000-0002-7781-1616

Author Contributions

⊥K.P.S. and W.E.R. contributed equally.

Notes

The authors declare no competing financial interest.

Additional data related to this publication are available at the University of Cambridge data repository (https://doi.org/10.17863/CAM.32922).

■ ACKNOWLEDGMENTS

This work was supported by an ERC Consolidator Grant "MatEnSAP" (682833 to E.R.), the U.K. Engineering and Physical Sciences Research Council (EP/L015978/1 and EP/G037221/1, nanoDTC to W.E.R., and a DTA studentship to K.P.S.), the Christian Doppler Research Association (Austrian Federal Ministry for Digital and Economic Affairs and the National Foundation for Research, Technology and Development), the OMV group (to E.R. and J.W.), the Cluster of Excellence RESOLV (EXC 1069) funded by the Deutsche Forschungsgemeinschaft (to A.R. and M.M.N.), the European Union's Horizon 2020 MSCA ITN-EJD 764920 PHOTOBIOCAT (to M.M.N.), Fundação para a Ciência e Tecnologia (Portugal) fellowship SFRH/BD/116515/2016 (to A.R.O.), grant PTDC/BIA-MIC/2723/2014 (to I.A.C.P.) and R&D units UID/Multi/04551/2013 (Green-IT), and LISBOA-01-0145-FEDER-007660 (MostMicro) cofunded by FCT/MCTES and FEDER funds through COMPETE2020/POCI and European Union's Horizon 2020 research and innovation programme (grant agreement no. 810856). We thank Mr. Andreas Wagner, Mr. Charles Creissen, and Dr. Judy Hirst for fruitful discussions.

■ REFERENCES

(1) Bassham, J. A.; Benson, A. A.; Kay, L. D.; Harris, A. Z.; Wilson, A. T.; Calvin, M. The Path of Carbon in Photosynthesis. XXI. The Cyclic Regeneration of Carbon Dioxide Acceptor. *J. Am. Chem. Soc.* **1954**, *76*, 1760–1770.

(2) Barber, J.; Tran, P. D. From Natural to Artificial Photosynthesis. *J. R. Soc., Interface* **2013**, *10*, 20120984.

(3) Kruse, O.; Rupprecht, J.; Mussgnug, J. H.; Dismukes, G. C.; Hankamer, B. Photosynthesis: A Blueprint for Solar Energy Capture and Biohydrogen Production Technologies. *Photochem. Photobiol. Sci.* **2005**, *4*, 957–969.

(4) Walker, B. J.; VanLoocke, A.; Bernacchi, C. J.; Ort, D. R. The Costs of Photorespiration to Food Production Now and in the Future. *Annu. Rev. Plant Biol.* **2016**, *67*, 107–129.

(5) Erb, T. J.; Zarzycki, J. A Short History of RubisCO: The Rise and Fall (?) Of Nature's Predominant CO_2 Fixing Enzyme. *Curr. Opin. Biotechnol.* **2018**, *49*, 100–107.

(6) Cotton, C. A.; Edlich-Muth, C.; Bar-Even, A. Reinforcing Carbon Fixation: CO_2 Reduction Replacing and Supporting Carboxylation. *Curr. Opin. Biotechnol.* **2018**, *49*, 49–56.

(7) Ragsdale, S. W.; Pierce, E. Acetogenesis and the Wood-Ljungdahl Pathway of CO_2 Fixation. *Biochim. Biophys. Acta, Proteins Proteomics* **2008**, *1784*, 1873–1898.

(8) Kebeish, R.; Niessen, M.; Thiruveedhi, K.; Bari, R.; Hirsch, H. J.; Rosenkranz, R.; Stäbler, N.; Schönfeld, B.; Kreuzaler, F.; Peterhänsel, C. Chloroplastic Photorespiratory Bypass Increases Photosynthesis and Biomass Production in Arabidopsis Thaliana. *Nat. Biotechnol.* **2007**, *25*, 593–599.

(9) Keller, M. W.; Schut, G. J.; Lipscomb, G. L.; Menon, A. L.; Iwuchukwu, I. J.; Leuko, T. T.; Thorgersen, M. P.; Nixon, W. J.; Hawkins, A. S.; Kelly, R. M.; Adams, M. W. W. Exploiting Microbial Hyperthermophilicity to Produce an Industrial Chemical, Using Hydrogen and Carbon Dioxide. *Proc. Natl. Acad. Sci. U. S. A.* **2013**, *110*, 5840–5845.

(10) Mattozzi, M. d.; Ziesack, M.; Voges, M. J.; Silver, P. A.; Way, J. C. Expression of the Sub-Pathways of the Chloroflexus Aurantiacus 3-Hydroxypropionate Carbon Fixation Bicycle in E. Coli: Toward Horizontal Transfer of Autotrophic Growth. *Metab. Eng.* **2013**, *16*, 130–139.

(11) Shih, P. M.; Zarzycki, J.; Niyogi, K. K.; Kerfeld, C. A. Introduction of a Synthetic CO_2-Fixing Photorespiratory Bypass into a Cyanobacterium. *J. Biol. Chem.* **2014**, *289*, 9493–9500.

(12) Kreel, N. E.; Tabita, F. R. Serine 363 of a Hydrophobic Region of Archaeal Ribulose 1,5-Bisphosphate Carboxylase/Oxygenase from Archaeoglobus Fulgidus and Thermococcus Kodakaraensis Affects CO_2/O_2 Substrate Specificity and Oxygen Sensitivity. *PLoS One* **2015**, *10*, e0138351.

(13) Antonovsky, N.; Gleizer, S.; Noor, E.; Zohar, Y.; Herz, E.; Barenholz, U.; Zelcbuch, L.; Amram, S.; Wides, A.; Tepper, N.; et al. Sugar Synthesis from CO_2 in Escherichia Coli. *Cell* **2016**, *166*, 115–125.

(14) Yu, H.; Li, X.; Duchoud, F.; Chuang, D. S.; Liao, J. C. Augmenting the Calvin-Benson-Bassham Cycle by a Synthetic Malyl-CoA-Glycerate Carbon Fixation Pathway. *Nat. Commun.* **2018**, *9*, 2008.

(15) Schwander, T.; Schada von Borzyskowski, L.; Burgener, S.; Cortina, N. S.; Erb, T. J. A Synthetic Pathway for the Fixation of Carbon Dioxide in Vitro. *Science* **2016**, *354*, 900–904.

(16) Tu, W.; Zhou, Y.; Zou, Z. Photocatalytic Conversion of CO_2 into Renewable Hydrocarbon Fuels: State-of-the-Art Accomplishment, Challenges, and Prospects. *Adv. Mater.* **2014**, *26*, 4607–4626.

(17) Montoya, J. H.; Seitz, L. C.; Chakthranont, P.; Vojvodic, A.; Jaramillo, T. F.; Nørskov, J. K. Materials for Solar Fuels and Chemicals. *Nat. Mater.* **2017**, *16*, 70–81.

(18) Loges, B.; Boddien, A.; Junge, H.; Beller, M. Controlled Generation of Hydrogen from Formic Acid Amine Adducts at Room Temperature and Application in H_2/O_2 Fuel Cells. *Angew. Chem., Int. Ed.* **2008**, *47*, 3962–3965.

(19) Kuehnel, M. F.; Wakerley, D. W.; Orchard, K. L.; Reisner, E. Photocatalytic Formic Acid Conversion on CdS Nanocrystals with Controllable Selectivity for H_2 or CO. *Angew. Chem., Int. Ed.* **2015**, *54*, 9627–9631.

(20) Graentzdoerffer, A.; Rauh, D.; Pich, A.; Andreesen, J. R. Molecular and Biochemical Characterization of Two Tungsten-and Selenium-Containing Formate Dehydrogenases from Eubacterium Acidaminophilum That Are Associated with Components of an Iron-Only Hydrogenase. *Arch. Microbiol.* **2003**, *179*, 116–130.

(21) Reda, T.; Plugge, C. M.; Abram, N. J.; Hirst, J. Reversible Interconversion of Carbon Dioxide and Formate by an Electroactive Enzyme. *Proc. Natl. Acad. Sci. U. S. A.* **2008**, *105*, 10654–10658.

(22) Hartmann, T.; Leimkühler, S. The Oxygen-Tolerant and NAD^+-Dependent Formate Dehydrogenase from Rhodobacter Capsulatus Is Able to Catalyze the Reduction of CO_2 to Formate. *FEBS J.* **2013**, *280*, 6083–6096.

DOI: 10.1021/jacs.8b10247
J. Am. Chem. Soc. 2018, 140, 16418–16422

(23) Schuchmann, K.; Müller, V. Direct and Reversible Hydrogenation of CO_2 to Formate by a Bacterial Carbon Dioxide Reductase. *Science* **2013**, *342*, 1382−1385.
(24) Bassegoda, A.; Madden, C.; Wakerley, D. W.; Reisner, E.; Hirst, J. Reversible Interconversion of CO_2 and Formate by a Molybdenum-Containing Formate Dehydrogenase. *J. Am. Chem. Soc.* **2014**, *136*, 15473−15476.
(25) Maia, L. B.; Fonseca, L.; Moura, I.; Moura, J. J. G. Reduction of Carbon Dioxide by a Molybdenum-Containing Formate Dehydrogenase: A Kinetic and Mechanistic Study. *J. Am. Chem. Soc.* **2016**, *138*, 8834−8846.
(26) Yu, X.; Niks, D.; Mulchandani, A.; Hille, R. Efficient Reduction of CO_2 by the Molybdenum-Containing Formate Dehydrogenase from Cupriavidus Necator (Ralstonia Eutropha). *J. Biol. Chem.* **2017**, *292*, 16872−16879.
(27) Sakai, K.; Kitazumi, Y.; Shirai, O.; Takagi, K.; Kano, K. Direct Electron Transfer-Type Four-Way Bioelectrocatalysis of CO_2/Formate and NAD^+/NADH Redox Couples by Tungsten-Containing Formate Dehydrogenase Adsorbed on Gold Nanoparticle-Embedded Mesoporous Carbon Electrodes Modified with 4-Mercaptopyridine. *Electrochem. Commun.* **2017**, *84*, 75−79.
(28) Robinson, W. E.; Bassegoda, A.; Reisner, E.; Hirst, J. Oxidation-State-Dependent Binding Properties of the Active Site in a Mo-Containing Formate Dehydrogenase. *J. Am. Chem. Soc.* **2017**, *139*, 9927−9936.
(29) Yuan, M.; Sahin, S.; Cai, R.; Abdellaoui, S.; Hickey, D. P.; Minteer, S. D.; Milton, R. D. Creating a Low-Potential Redox Polymer for Efficient Electroenzymatic CO_2 Reduction. *Angew. Chem., Int. Ed.* **2018**, *57*, 6582−6586.
(30) Sahin, S.; Cai, R.; Milton, R. D.; Abdellaoui, S.; Macazo, F. C.; Minteer, S. D. Molybdenum-Dependent Formate Dehydrogenase for Formate Bioelectrocatalysis in a Formate/O_2 Enzymatic Fuel Cell. *J. Electrochem. Soc.* **2018**, *165*, 109−113.
(31) Sakai, K.; Kitazumi, Y.; Shirai, O.; Kano, K. Bioelectrocatalytic Formate Oxidation and Carbon Dioxide Reduction at High Current Density and Low Overpotential with Tungsten-Containing Formate Dehydrogenase and Mediators. *Electrochem. Commun.* **2016**, *65*, 31−34.
(32) Sakai, K.; Kitazumi, Y.; Shirai, O.; Takagi, K.; Kano, K. Efficient Bioelectrocatalytic CO_2 Reduction on Gas-Diffusion-Type Biocathode with Tungsten-Containing Formate Dehydrogenase. *Electrochem. Commun.* **2016**, *73*, 85−88.
(33) Kuwabata, S.; Tsuda, R.; Nishida, K.; Yoneyama, H. Electrochemical Conversion of Carbon Dioxide to Methanol with Use of Enzymes as Biocatalysts. *Chem. Lett.* **1993**, *22*, 1631−1634.
(34) Kuwabata, S.; Tsuda, R.; Yoneyama, H. Electrochemical Conversion of Carbon Dioxide to Methanol with the Assistance of Formate Dehydrogenase and Methanol Dehydrogenase as Biocatalysts. *J. Am. Chem. Soc.* **1994**, *116*, 5437−5443.
(35) Schlager, S.; Dumitru, L. M.; Haberbauer, M.; Fuchsbauer, A.; Neugebauer, H.; Hiemetsberger, D.; Wagner, A.; Portenkirchner, E.; Sariciftci, N. S. Electrochemical Reduction of Carbon Dioxide to Methanol by Direct Injection of Electrons into Immobilized Enzymes on a Modified Electrode. *ChemSusChem* **2016**, *9*, 631−635.
(36) Amao, Y.; Shuto, N. Formate Dehydrogenase−viologen-Immobilized Electrode for CO_2 Conversion, for Development of an Artificial Photosynthesis System. *Res. Chem. Intermed.* **2014**, *40*, 3267−3276.
(37) Hwang, H.; Yeon, Y. J.; Lee, S.; Choe, H.; Jang, M. G.; Cho, D. H.; Park, S.; Kim, Y. H. Electro-Biocatalytic Production of Formate from Carbon Dioxide Using an Oxygen-Stable Whole Cell Biocatalyst. *Bioresour. Technol.* **2015**, *185*, 35−39.
(38) Lee, S. Y.; Lim, S. Y.; Seo, D.; Lee, J. Y.; Chung, T. D. Light-Driven Highly Selective Conversion of CO_2 to Formate by Electrosynthesized Enzyme/Cofactor Thin Film Electrode. *Adv. Energy Mater.* **2016**, *6*, 1502207.
(39) Kim, S.; Kim, M. K.; Lee, S. H.; Yoon, S.; Jung, K. D. Conversion of CO_2 to Formate in an Electroenzymatic Cell Using Candida Boidinii Formate Dehydrogenase. *J. Mol. Catal. B: Enzym.* **2014**, *102*, 9−15.
(40) Srikanth, S.; Maesen, M.; Dominguez-Benetton, X.; Vanbroekhoven, K.; Pant, D. Enzymatic Electrosynthesis of Formate through CO_2 Sequestration/Reduction in a Bioelectrochemical System (BES). *Bioresour. Technol.* **2014**, *165*, 350−354.
(41) Nam, D. H.; Kuk, S. K.; Choe, H.; Lee, S.; Ko, J. W.; Son, E. J.; Choi, E. G.; Kim, Y. H.; Park, C. B. Enzymatic Photosynthesis of Formate from Carbon Dioxide Coupled with Highly Efficient Photoelectrochemical Regeneration of Nicotinamide Cofactors. *Green Chem.* **2016**, *18*, 5989−5993.
(42) Kim, S. H.; Chung, G. Y.; Kim, S. H.; Vinothkumar, G.; Yoon, S. H.; Jung, K. D. Electrochemical NADH Regeneration and Electroenzymatic CO_2 Reduction on Cu Nanorods/Glassy Carbon Electrode Prepared by Cyclic Deposition. *Electrochim. Acta* **2016**, *210*, 837−845.
(43) Miyatani, R.; Amao, Y. Bio-CO_2 Fixation with Formate Dehydrogenase from Saccharomyces Cerevisiae and Water-Soluble Zinc Porphyrin by Visible Light. *Biotechnol. Lett.* **2002**, *24*, 1931−1934.
(44) Amao, Y.; Takahara, S.; Sakai, Y. Visible-Light Induced Hydrogen and Formic Acid Production from Biomass and Carbon Dioxide with Enzymatic and Artificial Photosynthesis System. *Int. J. Hydrogen Energy* **2014**, *39*, 20771−20776.
(45) Ikeyama, S.; Amao, Y. A Novel Electron Carrier Molecule Based on a Viologen Derivative for Visible Light-Driven CO_2 Reduction to Formic Acid with the System of Zinc Porphyrin and Formate Dehydrogenase. *Sustain. Energy Fuels* **2017**, *1*, 1730−1733.
(46) Noji, T.; Jin, T.; Nango, M.; Kamiya, N.; Amao, Y. CO_2 Photoreduction by Formate Dehydrogenase and a Ru-Complex in a Nanoporous Glass Reactor. *ACS Appl. Mater. Interfaces* **2017**, *9*, 3260−3265.
(47) Tsujisho, I.; Toyoda, M.; Amao, Y. Photochemical and Enzymatic Synthesis of Formic Acid from CO_2 with Chlorophyll and Dehydrogenase System. *Catal. Commun.* **2006**, *7*, 173−176.
(48) Ihara, M.; Kawano, Y.; Urano, M.; Okabe, A. Light Driven CO_2 Fixation by Using Cyanobacterial Photosystem I and NADPH-Dependent Formate Dehydrogenase. *PLoS One* **2013**, *8*, e71581.
(49) da Silva, S. M.; Voordouw, J.; Leitão, C.; Martins, M.; Voordouw, G.; Pereira, I. A. C. Function of Formate Dehydrogenases in Desulfovibrio Vulgaris Hildenborough Energy Metabolism. *Microbiology* **2013**, *159*, 1760−1769.
(50) Sokol, K. P.; Robinson, W. E.; Warnan, J.; Kornienko, N.; Nowaczyk, M. M.; Ruff, A.; Zhang, J. Z.; Reisner, E. Bias-Free Photoelectrochemical Water Splitting with Photosystem II on a Dye-Sensitised Photoanode Wired to Hydrogenase. *Nat. Energy* **2018**, *3*, 944−951.
(51) Rosser, T. E.; Gross, M. A.; Lai, Y. H.; Reisner, E. Precious-Metal Free Photoelectrochemical Water Splitting with Immobilised Molecular Ni and Fe Redox Catalysts. *Chem. Sci.* **2016**, *7*, 4024−4035.
(52) Mersch, D.; Lee, C.-Y.; Zhang, J. Z.; Brinkert, K.; Fontecilla-Camps, J. C.; Rutherford, A. W.; Reisner, E. Wiring of Photosystem II to Hydrogenase for Photoelectrochemical Water-Splitting. *J. Am. Chem. Soc.* **2015**, *137*, 8541−8549.
(53) Sokol, K. P.; Mersch, D.; Hartmann, V.; Zhang, J. Z.; Nowaczyk, M. M.; Rögner, M.; Ruff, A.; Schuhmann, W.; Plumeré, N.; Reisner, E. Rational Wiring of Photosystem II to Hierarchical Indium Tin Oxide Electrodes Using Redox Polymers. *Energy Environ. Sci.* **2016**, *9*, 3698−3709.
(54) Leung, J. J.; Warnan, J.; Nam, D. H.; Zhang, J. Z.; Willkomm, J.; Reisner, E. Photoelectrocatalytic H_2 Evolution in Water with Molecular Catalysts Immobilised on p-Si via a Stabilising Mesoporous TiO_2 Interlayer. *Chem. Sci.* **2017**, *8*, 5172−5180.

DOI: 10.1021/jacs.8b10247
J. Am. Chem. Soc. 2018, 140, 16418−16422